

The impact of neutron star spin on X-ray spectra

M. J. Burke^{1*}, M. Gilfanov^{1,2,3} and R. Sunyaev^{1,2}

¹ *Max Planck Institute for Astrophysics, Karl-Schwarzschild-Str. 1, Garching b. Munchen D-85741, Germany*

² *Space Research Institute of Russian Academy of Sciences, Profsoyuznaya 84/32, 117997 Moscow, Russia*

³ *Kazan Federal University, Kremlevskaya str.18, 420008 Kazan, Russia*

Accepted Year Month Day. Received Year Month Day; in original form Year Month Day

ABSTRACT

We investigate whether the intrinsic spin of neutron stars leaves an observable imprint on the spectral properties of X-ray binaries. To evaluate this we consider a sample of nine NSs for which the spins have been measured that are not accreting pulsars (for which the accretion geometry will be different). For each source, we perform spectroscopy on a majority of RXTE hard state observations. Our sample of sources and observations spans the range of the Eddington ratios $L_X/L_{Edd} \sim 0.005 - 0.100$.

We find a clear trend between key Comptonization properties and the NS spin for a given accretion rate. Specifically, at a given L/L_{Edd} , for more rapidly rotating NSs we find lower seed photon temperatures and a general increase in Comptonization strength, as parametrised by the Comptonization y parameter and amplification factor A . This is in good agreement with the theoretical scenario whereby less energy is liberated in a boundary layer for more rapidly spinning NSs, resulting in a lower seed photon luminosity and, consequently, less Compton cooling in the corona. This effect in extremis results in the hard states of the most rapidly spinning sources encroaching upon the regime of Comptonization properties occupied by BHs.

Key words: circumstellar matter – infrared: stars.

1 INTRODUCTION

X-ray binaries (XBs) possess rapidly spinning neutron stars (NSs) that are ‘spun up’ by accretion, an idea that was initially motivated by the need to identify possible progenitors (Smarr & Blandford 1976; Bisnovatyi-Kogan & Komberg 1976) for pulsars with rotation periods in the millisecond regime (Hulse & Taylor 1975). The large collecting area and excellent timing capabilities of the RXTE spacecraft (Bradt et al. 1993) led to a variety of high frequency phenomena being discovered at X-ray energies, such as accreting millisecond pulsars (Wijnands & van der Klis 1998). Another early breakthrough saw the detection of millisecond oscillations during type-I X-ray bursts (Strohmayer et al. 1996), which are characterised by a rapid increase in the X-ray flux over a period of 1 – 10 seconds that subsequently decays over 0.1 – 10 minutes. Such bursts are the result of unstable thermonuclear burning of accreted material on the NS surface (Bildsten 1995; Strohmayer & Bildsten 2006). While the exact mechanism of the burst oscillations is still open for debate (see Watts 2012, for review), repeated observations over months and years show consistent frequencies and behaviour for those of any particular source (see Galloway et al. 2008, for review of burst proper-

ties). Consensus formed that the oscillations observed during bursts are the result of some anisotropy in the emission from the NS surface, an interpretation that was vindicated by discovery of burst oscillations from millisecond pulsars with frequencies within 6×10^{-3} Hz of the known rotation frequencies (Chakrabarty et al. 2003; Strohmayer et al. 2003). A sound understanding of NS spin and its effects will play a crucial role refining the NS equation of state (see overview by Miller & Lamb 2016), and has enormous potential for the emerging field of gravitational wave astrophysics (e.g. Bildsten 1998; Andersson et al. 2005; Messenger et al. 2015).

In our previous work (Burke et al. 2017, hereafter Paper I) we reported a possible connection between hard state spectral properties of NS XBs and their spin. This result was not conclusive, but pointed towards a simple picture of the effect of spin on the spectral shape. We found hints of a positive correlation between spin and the strength of Comptonisation, which we characterised in terms of the amplification A , the ratio of the total luminosity to the seed photon luminosity, and the Compton y -parameter, which is a measure of the average change in energy experienced by a population of photons travelling through a finite medium. Our interpretation is that accreting material surrenders more energy as it impacts upon less rapidly rotating NSs which in turn produces more soft seed photons for Comptoni-

* E-mail: mburke@mpa-garching.mpg.de (MJB);

sation leading to increased Comptonization losses for hot electrons, as proposed by Shakura & Sunyaev (1988) and Sunyaev & Titarchuk (1989).

The main result of Paper I is a dichotomy observed in the Comptonisation strength between hard state spectra of NS and BH XBs. Comptonisation in NSs is suppressed by additional seed photons that are produced in the vicinity of the NS surface, on the surface itself or in a boundary layer between the surface and geometrically thin accretion disc. Theoretically such a boundary layer forms to facilitate the change in angular momentum between the innermost portions of the disc and the surface (Shakura & Sunyaev 1988) giving rise to blackbody-like emission, which has been observed using Fourier-resolved spectroscopy of soft state spectra (Gilfanov et al. 2003; Revnivtsev & Gilfanov 2006). It is not clear whether the classical boundary layer exists during the hard state (see Done et al. 2007; Gilfanov 2010, for review) when the innermost portion of the accretion disc is thought to be truncated at many gravitational radii, however, there must still be some mechanism to bridge the difference in linear velocities between the accreting material and the neutron star surface. When the disc extends to the surface of the NS, at moderate accretion rates ($L/L_{Edd} \sim 0.1$), the scale height of the boundary layer is expected to be $\sim 1 - 2$ km, whereas at high L/L_{Edd} the scale height expands such that the NS is enveloped by accreting material (see Popham & Sunyaev 2001, fig. 1). However, in this work we consider only sources in the hard spectral state which roughly correspond to luminosities of $L/L_{Edd} \lesssim 0.1$.

In the Newtonian approximation the boundary layer contributes approximately 50% of the total source emission (Shakura & Sunyaev 1988). However, Sibgatullin & Sunyaev (1998) & Sibgatullin & Sunyaev (2000) showed that by considering realistic space time metrics the energy released by the boundary layer for a non-rotating NS is of order 70% of the total emission, and that this fraction decreases with increasing frequency of prograde rotation. In Paper I we estimated the emission from the vicinity of the NS as a fraction of the total emission to be in the range $\approx \frac{2}{3} - \frac{1}{2}$.

There are few concrete connections between spin frequencies and other observable quantities. Possible connections between the NS spin and the frequencies of the so-called kHz Quasi-periodic oscillations (QPOs) remain the most studied and debated proposition. kHz QPOs (van der Klis et al. 1996) are high frequency QPOs that are occasionally detected in pairs that vary in a correlated way (Barret et al. 2005) by tens to hundreds of Hz (see van der Klis 2006, for review of X-ray variability). Early studies noted that the measured difference in frequencies of the two kHz QPO was compatible with either the NS spin frequency or its half, depending on the source (van der Klis 2000; Psaltis 2001). This scenario is attractive in the context of beat frequency models, where the lower frequency QPO arises from the beat between the upper kHz QPO and spin frequency (Miller et al. 1998; Lamb & Miller 2001). However, other authors have argued that QPOs are actually a manifestation of the effects of strong gravity (e.g. Stella & Vietri 1999; Abramowicz et al. 2003; Zhang 2004; Stuchlík et al. 2008). Wang et al. (2014) plot 12 sources with measured kHz QPO pairs against spin, and conclude there is a ‘clustering with a high scatter’ around $\Delta\nu_{kHz} \approx$

$0.5\nu_{spin}$ and $\Delta\nu_{kHz} \approx \nu_{spin}$, but it is not clear whether there is a relationship. It was also found that the kHz-QPO frequency correlates with the X-ray flux and spectral shape as characterised by the position on the colour-colour diagram (Méndez et al. 1999; Barret 2001).

Muno et al. (2001) were the first to suggest different patterns of behaviour between ‘slow’ (≈ 300 Hz) and ‘fast’ (≈ 600 Hz) sources, noting that burst oscillations were almost always found during bursts exhibiting PRE for fast sources, whereas slower sources showed oscillations in all types of burst. In subsequent studies the picture proved to be more complicated; bursts with and without PRE are found from both slow and fast samples, but predominantly bursts containing oscillations are PRE bursts in the most rapidly rotating systems, and non-PRE bursts for other sources (Muno et al. 2004; Galloway et al. 2008). In addition to this, Galloway et al. (2008) found that burst durations are consistently short for slow sources, while the bursts for faster sources tend to have longer durations. Piro & Bildsten (2007) suggest that predominantly shorter bursts from more slowly rotating NSs could be a result of the greater velocity differential between the NS surface and the infalling material leading to greater mixing between the ashes of burned material and that which is freshly accreted, exhausting H and leading to faster, H-rich bursts. On the other hand, slow rotators could be accreting from companions that happen to be degenerate, which is why the burning material is lacking in H, and if confirmed would indicate a different evolutionary path for differently spinning sources (Galloway et al. 2008).

In this paper we set out to identify possible links between the persistent hard state spectra of NS XBs and their spin. In doing so we build upon the work of Paper I, first expanding our sample of NSs of known spin and the number of spectra for each source, and then by comparing their behaviour as a function of accretion rate. It may be worth noting that the effects we report here are unrelated to the GR effect of the NS spin similar to the effect of the BH spin on X-ray spectral formation in the vicinity of Kerr black hole. Rather, these effects are a result of the dependence of the energy released in the boundary layer on the velocity difference between the accreting material and the NS surface. Although accurate quantitative prediction of these effects requires knowledge of the precise metrics of the space-time in the vicinity of the neutron star (Sibgatullin & Sunyaev 1998), they can be understood in terms of Newtonian mechanics through the well known formula

$$L_{bl} = \frac{1}{2} \dot{M} (\alpha v_K - v_{NS})^2 \quad (1)$$

where αv_K is velocity of the in falling material expressed in terms of the Keplerian velocity v_K near the NS surface, the factor α (≤ 1) accounts for the possibility that in the hard state the accreting material can arrive at the stellar surface with sub-Keplerian velocity, and v_{NS} is linear velocity of the NS surface (Shakura & Sunyaev 1988; Kluzniak 1988).

2 SAMPLE SELECTION

To add additional sources to our sample we choose to consider only those for which the NS spin frequency is well

Source	N_H 10^{22} cm^{-2}	Spin Hz	F_{peak} $10^{-9} \text{ erg s}^{-1} \text{ cm}^{-2}$
4U 1608-52	1.81	620	132
GS 1826-238	0.171	611	33
SAX J1750.8-2900	4.3*	601	49.2
4U 1636-536	0.27	581	64
Aql X-1	0.28	550	89
KS 1731-260	0.31	524	43
4U 0614+09	0.448	415	200
4U 1728-33	1.24	363	84
4U 1702-429	1.12	329	76
4U 1705-44	0.67	298**	39.3

Table 1. Source Properties. For our spectral analysis we use equivalent Hydrogen column densities N_H inferred from 21 cm emission (Kalberla et al. 2005), except in the case of SAX J1750.8-2900 (*see § 3.1). The mean peak fluxes F_{peak} of X-ray bursts are those reported by Galloway et al. (2008) except for GS 1826-238 for which we use figures reported by Galloway et al. (2004) (see § 3) and for 4U 0614+09 (Kuulkers et al. 2010). Spin frequencies correspond to burst oscillation frequencies presented by Galloway et al. (2008) and Strohmayer et al. (2008) (in the case of 4U 0614+09). **For 4U 1705 – 44 we quote the difference in kHz QPO frequencies as an approximation of the true spin frequency (Ford et al. 1998), baring in mind the possible uncertainties inherent to this method of spin determination (Wang et al. 2014).

determined. This limits our considerations to only those sources for which oscillations have been observed during thermonuclear bursts (see Galloway et al. 2008), which we further refine by excluding millisecond pulsars, as these will almost certainly obey a different accretion geometry from non-pulsing XBs (see Patruno & Watts 2012, for review). We note that burst oscillations have only been detected once in the case of GS 1826-238 (Thompson et al. 2005), despite many bursts having been observed over the course of the RXTE lifetime. We discuss this source in more detail in §4. The sample was further reduced by observational constraints, such as sources that were too faint (such as MXB 1659 – 298) or are not observed in a hard state. At this stage we were left with 8 sources out of 10 LMXBs with coherent pulsations detected during the X-ray bursts but not in their persistent emission (Watts 2012), and Aql X-1 (which once displayed coherent oscillations in its persistent emission over a period of ≈ 100 s, Zhang et al. 1998). We include 4U 1705 – 44 from Paper I for completeness, despite no burst oscillations having been detected from this source, with a view to excluding it for analysis from which we seek to make firm conclusions about spin. We list our final sample, with their pertinent properties in table 1. We reduce all hard state datasets, which we define as those data possessing a mean hardness ratio ≥ 2 using the intensities measured in the 7.50 – 18.50 keV and 4.0 – 6.0 keV bands. We present the final list of observations in tables 2 & 3.

3 DATA REDUCTION AND ANALYSIS

We extract PCA and HEXTE spectra of each source as detailed in Paper I, taking care to remove any contamination by X-ray bursts. For complete consistency, we consider PCA data from PCU2 from each source and HEXTE data from cluster B only. We fit the spectra with an ab-

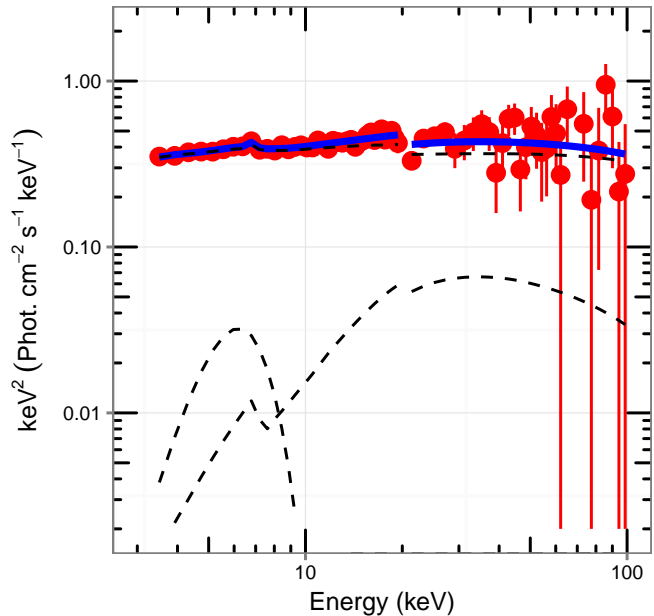


Figure 1. Example of unfolded spectral fit (blue line) using data from 4U 1608 – 52 (red). For illustration purposes we show the respective contributions of Comptonised and reflected emission, as well as that of the Gaussian component. For clarity, the emission from the Galactic ridge is omitted.

sorbed Comptonisation model with an additional Gaussian component to model the fluorescent Fe emission. In the spectral fitting package *Xspec*, this model takes the form of `CONST(PHABS(COMPPS+GAUSS))`, within which `COMPPS` models the Comptonised emission and its reflection by material in the accretion disc. As this work concerns the nature of NSs exclusively, we adjust the model from the approach in Paper I such as to have a blackbody-shaped seed photon spectrum, which is the same as the *Xspec* model `BBODYRAD`.

We model emission from the Galactic ridge (GR) as an additional set of fixed components comprising a $\Gamma = 2$ powerlaw and zero-width Gaussian that peaks at an energy of 6.6 keV (Revnivtsev 2003), the flux of which we calculate using the relation of Revnivtsev et al. (2006). As noted in Paper I, the close proximity of 4U 1728 – 33 to the Galactic centre means that there should be a substantial contribution of GR emission to these spectra. In this work we consider an additional two datasets from earlier in the RXTE mission, when the source was less luminous. On attempting to fit these spectra we noticed clear residual excesses in the spectral model at energies consistent with the line from GR emission, and unusual residuals at lower energies. This is clearly indicative that we have over-compensated for the GR emission in this source. To obtain our best estimate of the strength of GR in this instance, we perform a joint fit using all the spectra of 4U 1728 – 33, with the GR flux as the only tied parameter and with the GR spectral shape fixed. We recover a value of $3.2 \times 10^{-11} \text{ erg cm}^{-2} \text{ s}^{-1}$, just over half of our original estimate of $6.15 \times 10^{-11} \text{ erg cm}^{-2} \text{ s}^{-1}$, which we use in all subsequent analysis. In figure 1 we show an

Source	Proposal ID	Observation Suffix
4U 0614+09	50031	-01-01-06 -01-02-00 -01-02-02 -01-02-02 -01-02-02 -01-02-04 -01-02-04 -01-02-05 -01-02-05 -01-02-07 -01-05-00 -01-05-00 -01-05-00 -01-05-00 -01-05-01 -01-05-02 -01-05-02 -01-04-01
		-01-04-02 -01-04-03 -01-04-07 -01-04-04 -01-04-14 -01-04-15 -01-04-05 -01-04-06 -01-04-06
		-01-04-06 -01-04-08 -01-04-09 -01-04-09 -01-04-00 -01-04-00 -01-04-00 -01-04-00 -01-04-10
		-01-04-11 -01-04-16 -01-04-17 -01-04-18 -01-04-12 -01-04-13 -01-04-13 -01-04-13
		60424 -01-02-00 -01-02-00 -01-02-01
		70014 -04-01-00 -04-01-00 -04-01-01
		70015 -03-01-00 -03-01-00 -03-01-01 -03-02-00
		80037 -01-12-00
		80414 -01-01-01 -01-01-01 -01-03-00
		90422 -01-03-00
		92411 -01-09-00
		4U 1608-52
40437 -01-02-00		
50052 -01-33-00 -01-37-00		
60052 03-01-06 03-02-02 03-02-04 03-02-06		
70058 -01-01-00 -01-02-00 -01-04-00 -01-04-01 -01-05-00 -01-06-00 -01-10-00 -01-11-00 -01-12-00 -01-13-00		
91405 -01-14-01 -01-15-01 -01-16-00 -01-18-00 -01-20-00 -01-24-01 -01-25-00 -01-25-01 -01-26-00 -01-26-02		
-01-28-00 -01-28-01 -01-29-01 -01-30-00 -01-35-00 -01-35-01 -01-38-01 -01-39-00 -01-39-01		
-01-40-00 -01-40-01 -01-40-03		
4U 1636-536	90409	-01-01-00
		91024 -01-06-00 -01-07-00 -01-08-00 -01-09-00 -01-26-00 -01-27-00 -01-44-00 -01-51-00 -01-52-00 -01-72-00
		-01-73-00 -01-73-00 -01-74-00 -01-75-00 -01-76-00 -01-77-00 -01-97-00 -01-21-10 -01-22-10
		-01-23-10 -01-24-10 -01-25-10 -01-47-10 -01-48-10 -01-50-10 -01-68-10 -01-72-10 -01-11-00
		-01-78-01
		92023 -01-06-00 -01-06-01 -02-08-00 -01-08-00 -02-09-00 -02-10-00 -02-11-00 -01-11-00 -02-12-00 -01-12-00
-01-30-00 -01-31-00 -01-32-00 -01-33-00 -01-34-00 -01-35-00 -01-56-00 -01-57-00 -01-58-00		
-01-59-00 -01-97-00 -01-98-00 -01-01-10 -01-02-10 -01-20-10 -01-46-10 -01-50-10 -01-05-20		
-01-14-20 -01-15-20 -01-17-20 -01-18-20 -01-86-10 -01-49-10 -01-88-10		
4U 1702-429	40025	-04-03-01 -04-02-00
		50030 -01-05-00 -01-10-02 -01-10-02 -01-10-03 -01-10-03 -01-13-01 -01-13-02 -01-13-02
		80033 -01-01-01 -01-01-01 -01-21-02 -01-21-02 -01-20-01 -01-20-01 -01-20-04 -01-20-04
4U 1705-44	20073	-04-01-00
		40034 -01-08-02 -01-09-04 -01-09-01 -01-09-07
		40051 -03-10-00 -03-12-00 -03-12-00 -03-13-00
		91039 -01-01-41 -01-01-42 -01-01-43 -01-01-50 -01-01-51 -01-01-61

Table 2. RXTE Observations 1

example best-fit of our model to a spectrum from 4U 1608-52.

To explore the parameter space we make use of Bayesian X-ray Analysis software (BXA, Buchner et al. 2014) that connects nested sampling algorithm MultiNest (Feroz et al. 2009) to *Xspec*. We bin samples from the posterior distribution produced by BXA for a given spectrum to produce 1D and 2D confidence regions in a given parameter space. We measure the 3.0–200.0 keV flux for every point in each posterior chain, and calculate the Compton amplification factor A as a ratio of the total luminosity L_{Tot} ($= 4\pi f_{3-200} D^2$) to the seed photon luminosity L_{BB} ($= 4\pi R_{BB}^2 \sigma k T_{BB}^4$, where $R_{BB}^2 = N(D/10 \text{ kpc})^2$). As both L_{Tot} and L_{BB} are proportional to the distance squared, A is actually a distance independent quantity.

Finally, to calculate the luminosity as a fraction of Eddington luminosity we take the ratio of the measured 3–200 keV flux to the peak flux of type-I X-ray bursts (table 1) that exhibit PRE, when a source is presumed to be emitting at the Eddington luminosity L_{Edd} . This ratio, which we hence-

forth refer to as L/L_{Edd} , can be considered an excellent proxy for the accretion rate of the source and is a particularly convenient tool for discussing the luminosity of Galactic sources because it negates the need to involve source distances, which are often subject to various uncertainties. We note that for GS 1826 – 238 PRE bursts were not detected during the RXTE era, however, the type-I X-ray bursts from this source had a remarkably consistent profile with an average peak flux $33 \times 10^{-9} \text{ erg s}^{-1} \text{ cm}^{-2}$ (Galloway et al. 2004). A recent investigation by Chenevez et al. (2016) using NuSTAR data found evidence for PRE in one burst, with peak bolometric flux of $40 \pm 3 \times 10^{-9} \text{ erg s}^{-1} \text{ cm}^{-2}$, however, in the interests in consistency across the source sample we will use the RXTE-era value in our calculation of L/L_{Edd} .

3.1 SAX J1750.8-2900

The line-of-sight absorption column to SAX J1750.8-2900 is not well-known. The HEASoft N_H tool, which uses the 21 cm survey of Kalberla et al. (2005), displays a wide

Source	Proposal ID	Observation Suffix
4U 1728-33	10073	-01-10-00
	40027	-06-01-00 -06-01-02 -06-01-06 -06-01-03 -06-01-03 -06-01-03 -06-01-08 -08-02-01 -06-01-01 -06-01-01 -06-01-02 -06-01-04 -06-01-05
	91023	-01-06-00 -01-06-00
	92023	-03-47-10 -03-48-00 -03-49-00 -03-67-00 -03-69-00 -03-66-10 -03-83-10
Aql X-1	20092	-01-01-02 -01-02-02
	40033	-10-01-00 -10-01-01 -10-01-01 -10-01-02 -10-01-02 -10-01-02
	40048	-01-03-00 -01-03-00 -01-03-00 -01-03-00 -01-07-00 -01-07-00 -01-07-00
	40049	-01-02-00 -01-02-01 -01-03-00 -01-03-00 -01-03-00
	40432	-01-02-00 -01-02-00 -01-03-00
	50049	-01-04-00 -01-04-01 -02-03-01
	70426	-01-01-00
	90017	-01-01-00 -01-01-02 -01-02-00 -01-02-01 -01-03-01 -01-04-00 -01-06-00 -01-06-01 -01-07-00 -01-08-00 -01-08-01 -01-08-02 -01-09-00 -01-09-02
	91028	-01-01-00 -01-03-00 -01-04-00 -01-05-00 -01-07-00
KS 1731-260	40025	-02-03-02 -02-04-00 -02-04-01 -02-05-00 -02-05-01 -02-02-00 -02-03-01
	50031	-02-01-00 -02-01-00 -02-01-00 -02-01-07 -02-01-09 -02-01-10 -02-01-11 -02-01-12 -02-01-01 -02-01-01 -02-01-01 -02-01-02 -02-01-02 -02-01-02 -02-01-02 -02-01-02 -02-01-03 -02-01-03 -02-01-03 -02-01-04 -02-01-04 -02-01-05 -02-01-05 -02-01-05 -02-01-05 -02-01-08 -02-02-04 -02-02-05 -02-02-05 -02-02-00
SAX J1750.8-2900	93432	-01-05-02 -01-05-04 -01-06-00
GS 1826-238	30060	-03-03-00 -03-03-00 -03-03-00
	50035	-01-01-00 -01-01-00 -01-01-02 -01-01-02 -01-01-02
	70025	-01-01-00 -01-01-00 -01-01-00 -01-01-00
	70044	-01-01-00 -01-01-00 -01-01-00 -01-01-05 -01-01-01 -01-01-02 -01-02-00 -01-02-02 -01-02-03 -01-03-00 -01-04-00 -01-04-00 -01-04-00
	80048	-01-01-02 -01-01-17 -01-01-11 -01-01-00 -01-01-00 -01-01-00 -01-01-01 -01-01-01 -01-01-13 -01-01-03 -01-01-03 -01-01-14 -01-01-05 -01-01-04 -01-01-04 -01-01-04 -01-01-07 -01-01-07
	80049	-01-01-00 -01-03-00 -01-03-00 -01-03-00 -01-03-01 -01-03-01 -01-03-01 -01-03-01 -01-03-02 -01-03-02 -01-03-03 -01-03-03 -01-04-00
	80105	-11-01-00 -11-01-00
	90043	-01-01-00 -01-01-00 -01-01-00 -01-01-04 -01-01-02 -01-01-02 -01-01-01 -01-01-01 -01-01-01 -01-01-01 -01-01-01 -01-01-03 -01-02-01 -01-02-02 -01-02-03 -01-03-00 -01-03-01 -01-03-01
	91017	-01-01-02 -01-01-01 -01-01-01 -01-01-01 -01-01-01 -01-01-00 -01-02-17 -01-02-05 -01-02-04 -01-02-00 -01-02-12 -01-02-13 -01-02-14 -01-02-01 -01-02-07 -01-02-06 -01-02-08 -01-02-10
	92031	-01-01-00 -01-01-02 -01-01-03 -01-01-04 -01-01-06 -01-01-06 -01-01-01 -01-01-07 -01-01-08 -01-01-09 -01-02-01 -01-02-05 -01-02-04 -01-02-03 -01-02-02 -01-02-00 -01-02-00 -01-02-00 -01-02-00
	92703	-01-01-01 -01-02-01 -01-02-02 -01-02-03 -01-02-03 -01-02-03 -01-03-01 -01-03-00 -01-03-03 -01-03-02 -01-04-00 -01-04-01 -01-04-02

Table 3. RXTE Observations 2

range of values from $0.5 - 1.6 \times 10^{22} \text{ cm}^{-2}$ and presents an average weighted value of $0.927 \times 10^{22} \text{ cm}^{-2}$. Consulting the literature, we find that Allen et al. (2015) discussed the value of N_H in some detail, and performed an analysis of several *Swift* spectra with the value of N_H tied between the fits. Their procedure obtained $N_H = 4.3 \times 10^{22} \text{ cm}^{-2}$, which is consistent with the model-dependent extremes of $2.5 - 6.0 \times 10^{22} \text{ cm}^{-2}$ found using BeppoSAX data (Natalucci et al. 1999) and $4.0 - 5.9 \times 10^{22} \text{ cm}^{-2}$ using XMM data (Lowell et al. 2012). In our analysis we therefore adopt $N_H = 4.3 \times 10^{22} \text{ cm}^{-2}$.

All hard state observations of this source were made during 2008. We have concerns about HEXTE data obtained during this epoch. We analysed two observations of the Crab nebula (93802-02-15-00,93802-02-16-00) taken in the same week as one of the SAX J1750.8-2900 datasets. Fitting with the standard absorbed ($N_H = 0.38 \times 10^{22} \text{ cm}^{-2}$) power law model gave a best fit $\chi^2_\nu = 100/82 \sim 1.23$ and $112/82 \sim 1.37$ whereas in earlier epochs χ^2_ν is typically < 0.9 . Inspection

of the fit residuals in this case shows that the HEXTE data form a slope in the fit residuals, with the model in excess of the data at low energy ($\approx 20 - 40 \text{ keV}$) and a deficient at higher energies ($\approx 50 - 65 \text{ keV}$). We choose not to utilise the HEXTE data during this epoch. To compensate for the lack of high energy coverage we include PCA data in the range $20.0 - 45.0 \text{ keV}$. Two potential problems with this approach are that the PCA is less-well calibrated at energies $> 20 \text{ keV}$, and that we might not be able to constrain the electron temperature if it is particularly high (i.e. if $kT_e > 50 \text{ keV}$, as in the case of 4U 1608-52). In terms of calibration, we note the work of García et al. (2014), who computed an epoch-dependent ‘correction curve’ for PCA spectra based on accumulated Crab observations. For data such as these SAX J1750.8-2900 observations, from later PCA epochs, the calibration is accurate to within 1% upto $\approx 31 \text{ keV}$ (compared to 3–4% in earlier epochs) and can underestimate the flux by 2–4% from 34–45 keV. The spectra of SAX J1750.8-2900 typically have 20 – 150 net counts per channel at en-

ergies > 35 keV, therefore calibration inaccuracies should have a negligible effect on our analysis.

4 RESULTS

In figure 2 we present key spectral properties as a function of L/L_{Edd} , with sources denoted by different colours. Each datum represents the mean posterior estimate of a single spectrum and the associated standard deviation. To aid our investigation into the effects of NS spin, we divide the sample into two broad spin frequency groups divided about the mean value of our sample, ≈ 500 Hz, and in figure 2 denote members of each group with circles and triangles respectively. We note that if the peak bolometric flux measured during a type-I X-ray burst showing signs of PRE from GS 1826-238 is accurate (Chenevez et al. 2016), the true L/L_{Edd} for this source will be at $\sim 82\%$ of the values shown, and emphasise that this change would not be significant enough change to alter our conclusions.

There are clear trends with L/L_{Edd} in all four main parameters characterising the Comptonized spectra. Formally, the correlations are extremely significant. For example, for the Comptonization parameter, the Spearman rank test indicates a compatibility with the null hypothesis $p_n < 2.2 \times 10^{-16}$ and a correlation of 0.85 between y and L/L_{Edd} . It is also clear that there is significant overlap for each parameter for sources with different spins. This is further illustrated by the posterior distributions for groups of low- and high-spin sources, figures 4, which discussed in detail below. However, figure 2 suggests differences in behaviour correlated with spin do exist at a given accretion rate. Specifically, the low frequency sources all occupy a higher kT_{BB} at a given L/L_{Edd} compared to sources that contain more rapidly rotating NSs. Likewise, the more slowly rotating NSs appear to have lower y and A .

To test these possible trends connected to source spin we compute for each source the luminosity resolved mean values of spectral parameters and quantiles of their distributions. Each element of the posterior chains for every spectrum was allocated a bin based on L/L_{Edd} , and then used to compute quantiles for each source if it has a significant presence (equivalent to one entire posterior) in a given flux bin. In figure 3 we plot these quantiles (25%, 50% and 75%) as a boxplot with each box representing one source for each flux bin, with the spin of each source indicated by the strength of shading.

Figure 3 shows that the distributions of kT_{BB} occupy higher values for the three most slowly rotating NSs in all flux bins. Moreover, these same sources have consistently lower y -parameter across the full L/L_{Edd} range, while more rapid rotators have increasingly large values with increasing accretion rate. The picture in terms of A is less clear cut, with some sources occupying a wider range of values. However, for a majority of flux bins a slow spinning source will have lower A and y than a more rapidly spinning source.

In figure 4 we present the one dimensional posterior distributions of kT_{BB} , y and A for low and high-spin sources in three broad L/L_{Edd} bins. For y and A these distributions are compared with the corresponding distributions for black holes from Paper I. These distributions complement figures 2 and 3 in illustrating the dichotomy between low

and high spin sources and their trends with the Eddington ratio. These will be further discussed in section 5.

We ask what is the probability that kT_{BB} will correctly rank the sources by spin when temperature is drawn from a uniform distribution for fixed L/L_{Edd} ? Considering all 10 sources, we can broadly consider to fall into three groups within which the sources overlap. This makes groups of two groups of three sources, and one group of four sources. What is the probability that that kT_{BB} can rank the spectra into such groups by chance? Assuming L/L_{Edd} is fixed, we generate 10 random values of kT_{BB} from a uniform distribution over the observed range of kT_{BB} at that point ($\approx 0.6 - 0.85$ keV), and repeat for a large number of iterations. We then ask how many times are the first three numbers lower than the next 4 numbers, and at the same time those numbers are lower than the final 3 numbers? This analysis suggests a uniform distribution would produce this ranking result by chance with the probability of $\approx 2.4 \times 10^{-4}$.

As mentioned in section 2, in the case of GS 1826 – 238 burst oscillations have only been reported once by Thompson et al. (2005) who analysed three RXTE observations that had been simultaneously observed with *Chandra* in their search. Their detection is unconfirmed in many other bursts from this source observed by RXTE. In particular, Watts (2012) suggested that the authors underestimated the number of search trials in arriving at their significance estimate. Given these considerations we assume that the burst frequency is unknown, so as to test the impact on our results of withdrawing GS 1826-238 from the sample (just as we excluded many other NS LMXBs with unknown or unconfirmed spins). Withdrawing this source does not affect our conclusion that the Comptonizing properties are a function of both the accretion rate and spin. More specifically, removing this source from fig.3 (i.e. the four purple boxes at L/L_{Edd} 0.65 – 0.95) does not affect the split between higher and lower spin sources. In fig.4, removing this source will only affect the bottom row of panels corresponding to highest L/L_{Edd} , with the only noticeable effect being the disappearance of the second peak of the turquoise histogram in the bottom left panel. This does not affect the existence of the bimodality in these distributions, neither does it change the false alarm probabilities computed above.

5 DISCUSSION AND CONCLUSIONS

We have performed a systematic study of a sample of NS LMXB hard state spectra to investigate possible trends between the spectral properties and the NS rotation frequency. To this end, we modelled the hard state spectra as Comptonization of blackbody seed photons on thermal electrons, and explored the available parameter space for this model using nested sampling. We note that our approach does not account for the effects of inclination (as the emission will be locally anisotropic), second-order reflection effects in both the disc and boundary layer caused by the photons from each other, or relativistic effects from the vicinity of the NS (see discussion in Lapidus & Sunyaev 1985).

Overall, spectral properties depend strongly on the Eddington luminosity ratio, with different sources and different observation of the same source following same dependence, albeit with large scatter. In addition, at the given

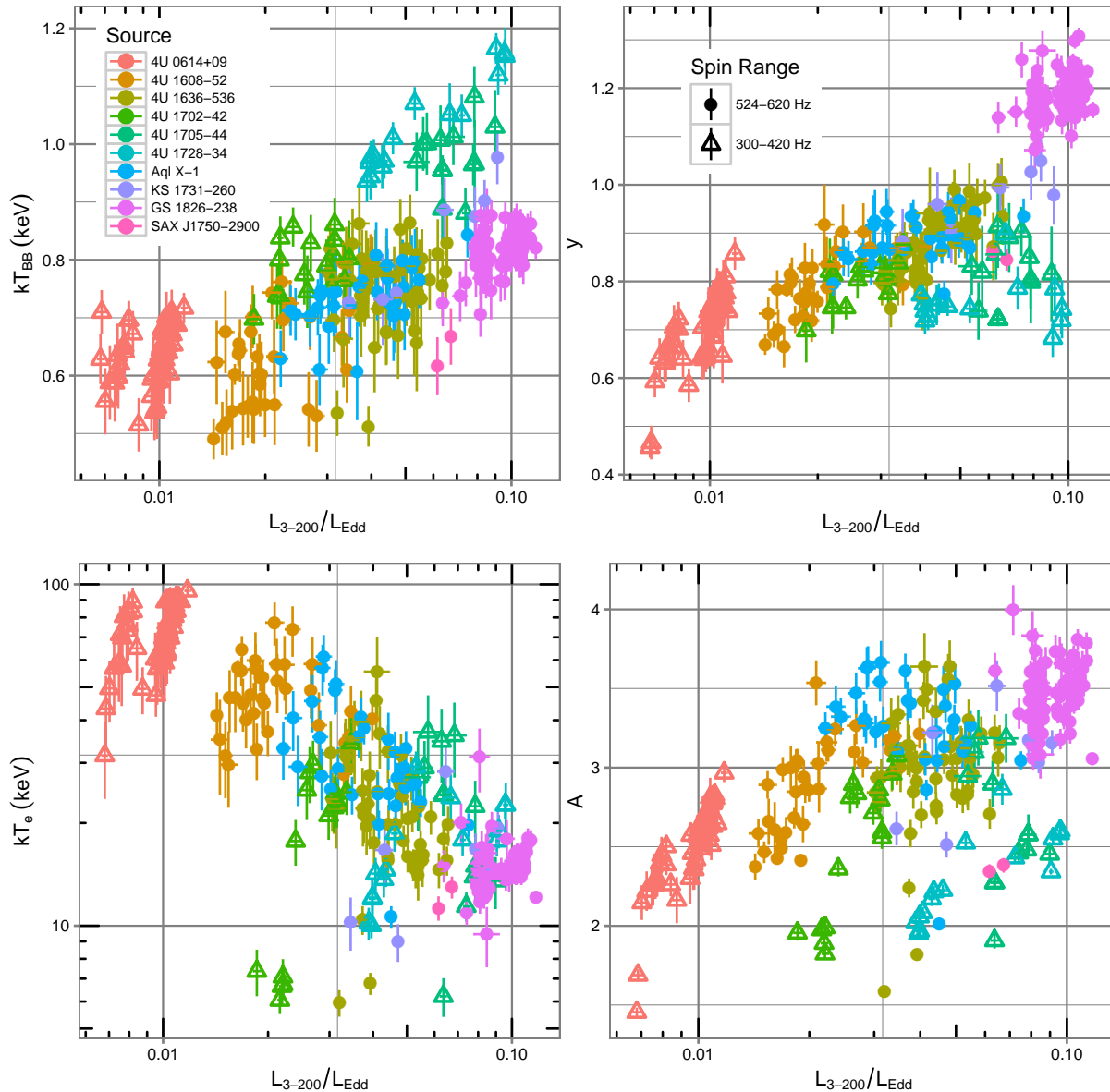


Figure 2. Variation of key spectral properties with L/L_{Edd} .

Eddington luminosity ratio (i.e. same mass accretion rate), there is a difference in spectral properties between different sources correlated with the NS rotation frequency. These differences are most apparent in terms of the seed photon temperature kT_{BB} and in the behaviour of the Compton y -parameter and Compton amplification factor A . Specifically, we find that at a given accretion rate the seed photon temperature is lower and Compton y -parameter and A are higher for more rapidly rotating NSs (figure 3). We do not find such a clear correlation with the NS spin in the case of the electron temperature kT_e .

For the standard Shakura-Sunyaev accretion disc around a slowly rotating NS, more than a half of the energy possessed by infalling material is released on the stellar surface (Shakura & Sunyaev 1988; Sibgatullin & Sunyaev 2000), in a narrow boundary or spreading layer

(Shakura & Sunyaev 1988; Inogamov & Sunyaev 1999, 2010) where the material decelerates between the Keplerian velocity of the disc and the rotational velocity of the NS surface. Analysis of Fourier-frequency-resolved spectra of multiple sources by Gilfanov et al. (2003) and Revnivtsev & Gilfanov (2006) suggests that in the soft spectral state, the boundary layer has an approximately blackbody spectrum of common characteristic temperature ≈ 2.4 keV. While no such spectral component has been identified in the NS hard state spectra, some fraction of the energy of the accreting matter is still expected to be released on the surface of the neutron star, in some form of boundary layer, but its emission is presumably intercepted by the Comptonizing material along the line-of-sight. Paper I showed that Comptonisation is generally weaker (smaller A & y) in NS systems than for their BH cousins

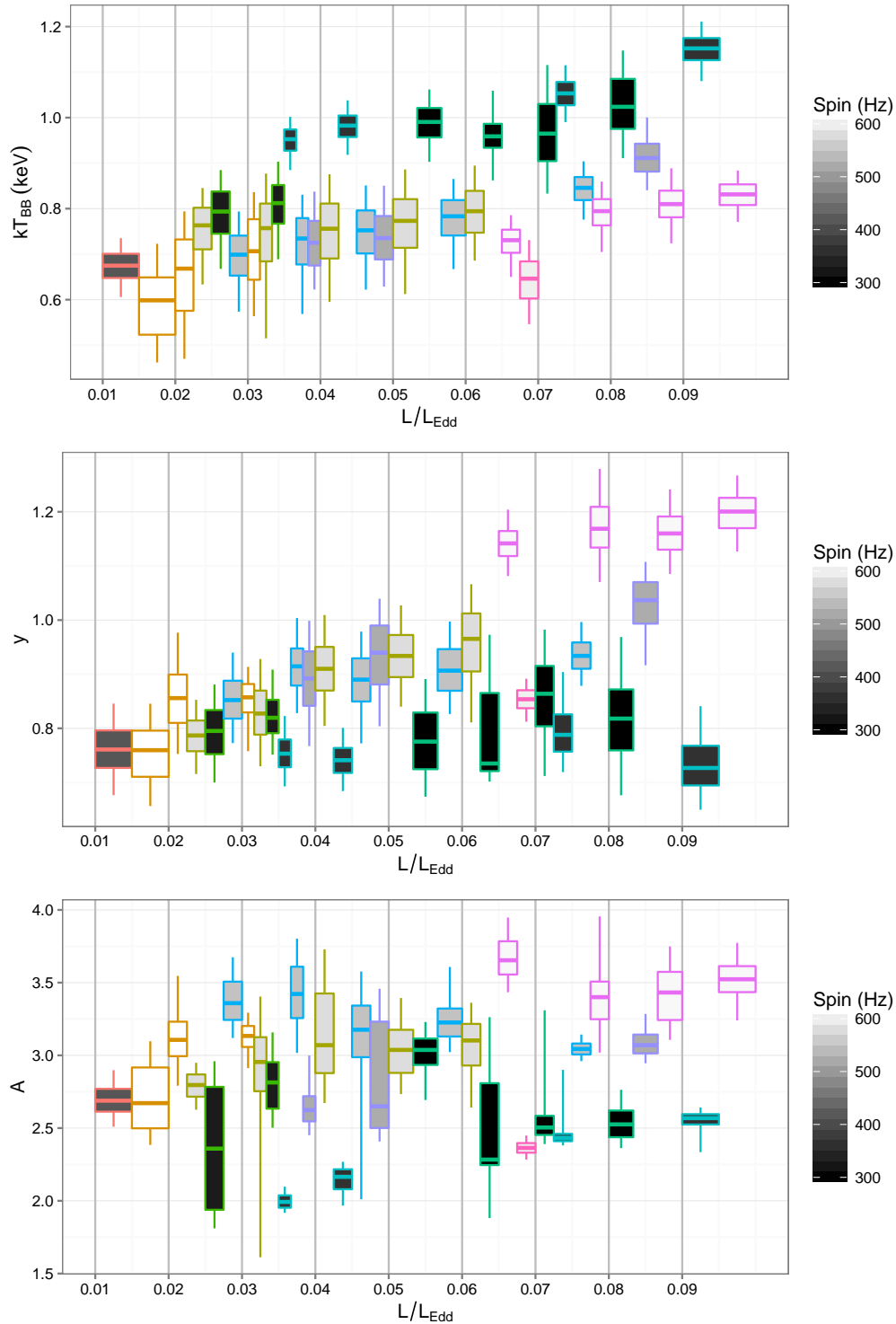


Figure 3. Comptonization model parameters binned by L/L_{Edd} , with grey vertical lines indicating the bin boundaries. Each box represents the weighted 25% – 75% interquartile range and each vertical line the 0.05 – 0.95% bounds for the distribution of that parameter across all posterior chain elements that fall in a given L/L_{Edd} bin for each source, with the line inside the box indicating the position of the median value. Boxes are offset in x for clarity.

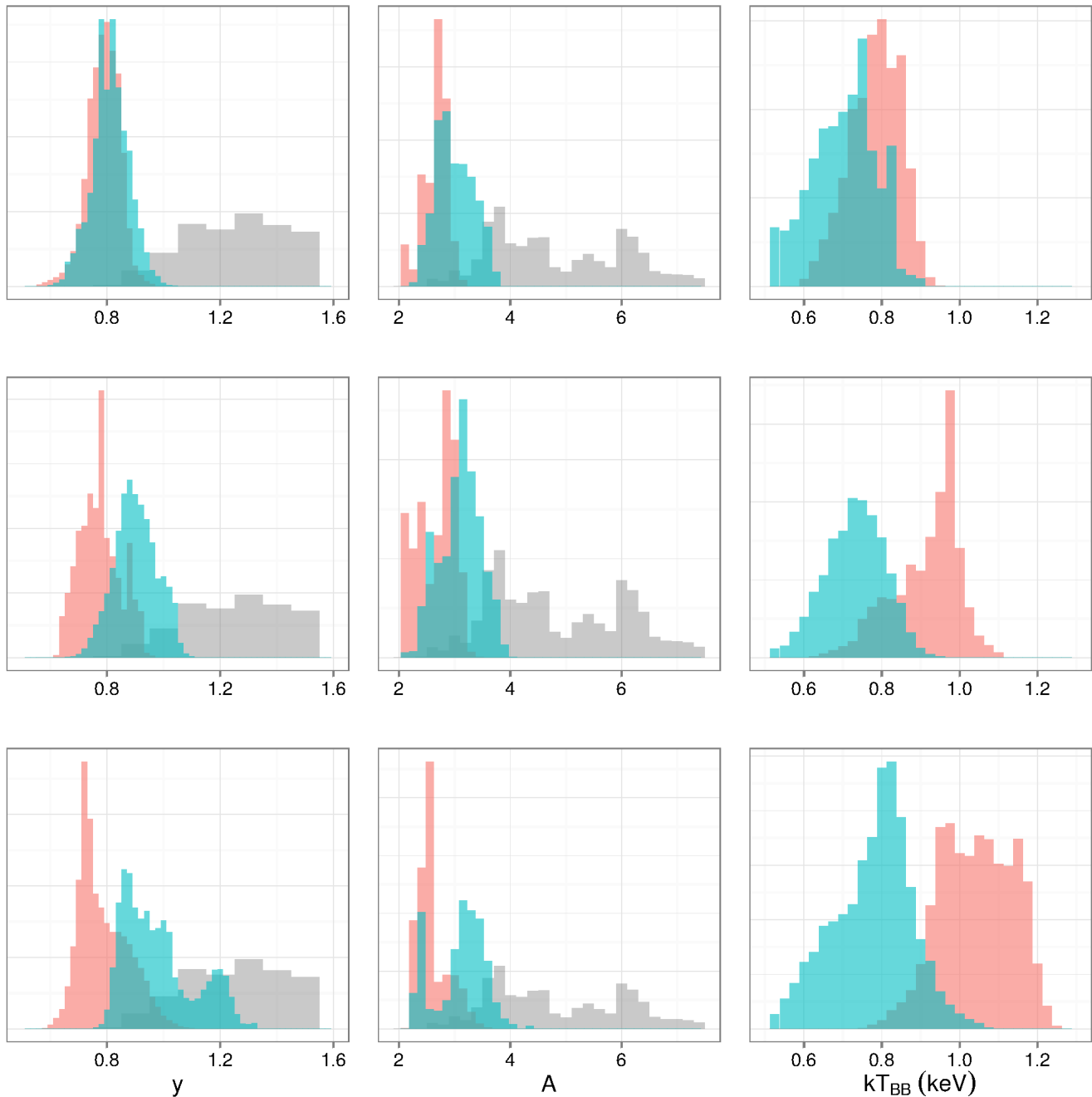


Figure 4. Flux-resolved posterior distributions of Compton y -parameter (left), Amplification factor A (center), and kT_{BB} (right) contrasting rapidly spinning NSs (> 500 Hz, turquoise) and more slowly rotating NSs (< 500 Hz, pink) with the equivalent distributions for BHs from Paper 1 (grey, left and centre only). Rows correspond to $L/L_{Edd} = 0.015 - 0.03$, $0.03 - 0.05$ and $0.05 - 0.10$ (top-bottom). BH distribution of y shifted by $+0.05$ (see text).

and this can be understood in terms of additional seed photons emitted by the neutron star instigating greater energy losses of hot electrons and reducing the Comptonizing strength of the corona. In Paper I we estimated that about $\sim 1/3 - 1/2$ of the accretion energy must be released on the surface of the neutron star in order to explain the difference in the parameters of the Comptonized spectra in BH and NS systems.

Gilfanov et al. (2003) and Revnivtsev & Gilfanov (2006) found that in the soft spectral state, the temperature of the spreading layer emission was of the order of the Eddington temperature¹ and did not depend on the mass accretion rate, which in their sample ranged from $\approx (0.1 - 1) \times L_{Edd}$. This result supported the theoretical

¹ ~ 2.5 keV for the distant observer, including colour correction, see Gilfanov & Sunyaev (2014) for details.

picture of the Eddington flux-limited levitating spreading layer supported by the radiation pressure, proposed earlier by Inogamov & Sunyaev (1999). In their model, the spectral shape of the boundary layer emission is determined only by the neutron star compactness (see Suleimanov & Poutanen 2006, for detailed calculation) and its luminosity is regulated by the surface area of the spreading layer. In the present work we find that in the hard spectral state on the contrary, the seed photon temperature is significantly smaller than the local Eddington value and varies with X-ray luminosity of the source, i.e. with the mass accretion rate. This points at the difference in the structure and dynamics of the boundary layer in the soft and hard spectral states.

The greater the differential between the linear velocity of the accreting material and that of the NS surface, the more energy is liberated at the boundary layer. In the Newtonian approximation the luminosity of the boundary layer L_{bl} is given by equation 1, which can be expressed in terms of the respective rotation frequencies f_K and f_{NS} ,

$$L_{bl} = 2\pi^2 \dot{M} R^2 (\alpha f_K - f_{NS})^2. \quad (2)$$

One can see from these equations that the luminosity of seed photon produced by the NS surface anti-correlates with the NS spin. For higher spin sources supply of the seed photons will be reduced resulting in stronger Comptonization, in particular in large Compton amplification factor A and Comptonization parameter y , in the same way as the dichotomy between BH and NS sources had been explained in Paper I.

Furthermore, assuming the emission from the boundary layer is well-approximated by a blackbody spectrum, then $L_{bl} \propto T^4$. This means that if all other factors (especially the emitting surface area) are similar across the population of NSs, the temperature of the seed photons $kT_{BB} \propto (\alpha f_K - f_{NS})^{\frac{1}{2}}$. The maximal Keplerian frequency in the accretion disc is of the order $f_K \sim 1.6 - 1.8$ kHz (Sibgatullin & Sunyaev 2000), while NS spins vary in the $f_{NS} \sim 0.3 - 0.6$ kHz range. At $L_X/L_{Edd} \sim 0.05$, the seed photon temperature varies from $kT_{BB} \sim 0.8 - 1.0$ keV, i.e. by a factor of about $\sim 1.2 - 1.3$, between low- and high-spin sources (Fig. 3). In order to explain such a difference between $f_{NS} \sim 0.3$ kHz and $f_{NS} \sim 0.6$ kHz sources, $\alpha \sim 0.7$ is required, which is broadly consistent with the conclusions of Paper I that the accreting material reaches the surface of the neutron star still possessing about $\sim 1/3 - 1/2$ of its initial energy.

5.1 Can fast spinning neutron stars mimic black holes?

From equation 2, at sufficiently high NS spin frequencies the luminosity of the boundary layer can become small. Theoretically, this can make accreting neutron stars similar to black holes from the point of view of the energy balance in the Comptonization region. Indeed, such a behaviour is evident in Figure 4 where the high-spin sources at high Eddington ratios progressively overlap with the region of Comptonization parameters, identified with black holes in Paper I. This dilutes the boundary between black holes and neutron stars. From Figure 2 one can see that three sources expand into $y \gtrsim 1.0$ regions at higher L/L_{Edd} : 4U 1636 – 536, KS 1731 – 260 and, most significantly, GS 1826 – 238. This

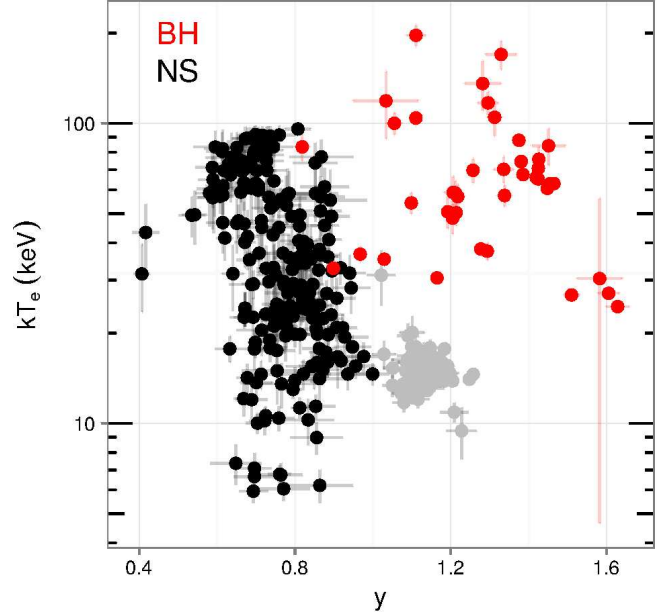


Figure 5. Compton y -parameter and kT_e for NS spectra from this work (black) and BH spectra from paper I (red). Points corresponding to GS 1826 – 238 are highlighted in grey (see discussion in §5.1).

behaviour is strongest at the highest Eddington ratios (but still compatible with the source being in the hard spectral state). All these sources have high spin (> 500 Hz), and their behaviour markedly contrasts with that of the slower sources at similar L/L_{Edd} , such as 4U 1728 – 34, the Comptonizing strength of which remains low. For GS 1826 – 238, which has one of the highest spins and mass accretion rates in our sample, the Comptonization parameter can reach values $y \sim 1.25$, which is inside the region occupied by BH LMXBs.² However, such high values of y are achieved only at high Eddington ratios, $L_X/L_{Edd} \sim 0.1$, at which neutron stars are characterised by extremely low electron temperature, $kT_e \sim 10 - 20$ keV (Figure 2), well below values typical for black holes (Fig. 5 in Paper I). This behaviour in $kT_e - y$ distinguishes NSs from black holes and is illustrated in figure 5. A detailed comparison of high spin neutron stars with black holes will be a subject of a separate study. As a final point, we mention that withdrawing GS 1826 – 238 from the sample (see discussion in §4) does not negate the encroachment of the more luminous and high-spin sources onto the territory of Comptonization strength occupied by BHs (Fig. 4), but makes it less extreme. This is illustrated in figure 5, where the GS 1826 – 238 points are shown in grey.

² We note that in the strictest sense these y should not be compared directly; the different seed photon model used in the current work means that we are in effect comparing two different models, however, experimentation by fitting the spectra in this work with both models shows that y is fairly resilient between both approaches, and on average y from using the blackbody seed photon spectrum is ≈ 0.05 higher than that recovered from fitting using a multicolour disc blackbody seed spectrum.

ACKNOWLEDGMENTS

Our sincere thanks to the anonymous referee, whose comments have improved the clarity of the paper. We acknowledge the use of the Legacy Archive for Microwave Background Data Analysis (LAMBDA), part of the High Energy Astrophysics Science Archive Center (HEASARC). HEASARC/LAMBDA is a service of the Astrophysics Science Division at the NASA Goddard Space Flight Center. MG acknowledges hospitality of the Kazan Federal University (KFU) and support by the Russian Government Program of Competitive Growth of KFU and RFBR grant No. 15-42-02573.

REFERENCES

- Abramowicz M. A., Bulik T., Bursa M., Kluźniak W., 2003, *A&A*, 404, L21
- Allen J. L., Linares M., Homan J., Chakrabarty D., 2015, *ApJ*, 801, 10
- Andersson N., Glampedakis K., Haskell B., Watts A. L., 2005, *MNRAS*, 361, 1153
- Barret D., 2001, *Advances in Space Research*, 28, 307
- Barret D., Kluźniak W., Olive J. F., Paltani S., Skinner G. K., 2005, *MNRAS*, 357, 1288
- Bildsten L., 1995, *ApJ*, 438, 852
- Bildsten L., 1998, *ApJL*, 501, L89
- Bisnovatyi-Kogan G. S., Komberg B. V., 1976, *Soviet Astronomy Letters*, 2, 130
- Bradt H. V., Rothschild R. E., Swank J. H., 1993, *A&AS*, 97, 355
- Buchner J., Georgakakis A., Nandra K., Hsu L., Rangel C., Brightman M., Merloni A., Salvato M., Donley J., Kocovski D., 2014, *A&A*, 564, A125
- Burke M. J., Gilfanov M., Sunyaev R., 2017, *MNRAS*, 466, 194
- Chakrabarty D., Morgan E. H., Muno M. P., Galloway D. K., Wijnands R., van der Klis M., Markwardt C. B., 2003, *Nature*, 424, 42
- Chenevez J., Galloway D. K., in 't Zand J. J. M., Tomsick J. A., Barret D., Chakrabarty D., Fürst F., Boggs S. E., Christensen F. E., Craig W. W., Hailey C. J., Harrison F. A., Romano P., Stern D., Zhang W. W., 2016, *ApJ*, 818, 135
- Done C., Gierliński M., Kubota A., 2007, *A&AR*, 15, 1
- Feroz F., Hobson M. P., Bridges M., 2009, *MNRAS*, 398, 1601
- Ford E. C., van der Klis M., Kaaret P., 1998, *ApJL*, 498, L41
- Galloway D. K., Cumming A., Kuulkers E., Bildsten L., Chakrabarty D., Rothschild R. E., 2004, *ApJ*, 601, 466
- Galloway D. K., Muno M. P., Hartman J. M., Psaltis D., Chakrabarty D., 2008, *ApJS*, 179, 360
- García J. A., McClintock J. E., Steiner J. F., Remillard R. A., Grinberg V., 2014, *ApJ*, 794, 73
- Gilfanov M., 2010, in Belloni T., ed., *The Jet Paradigm Vol. 794 of Lecture Notes in Physics*, Berlin Springer Verlag, X-Ray Emission from Black-Hole Binaries. p. 17
- Gilfanov M., Revnivtsev M., Molkov S., 2003, *A&A*, 410, 217
- Gilfanov M. R., Sunyaev R. A., 2014, *Physics Uspekhi*, 57, 377
- Hulse R. A., Taylor J. H., 1975, *ApJL*, 195, L51
- Inogamov N. A., Sunyaev R. A., 1999, *Astronomy Letters*, 25, 269
- Inogamov N. A., Sunyaev R. A., 2010, *Astronomy Letters*, 36, 848
- Kalberla P. M. W., Burton W. B., Hartmann D., Arnal E. M., Bajaja E., Morras R., Pöppel W. G. L., 2005, *A&A*, 440, 775
- Kluźniak W., 1988, PhD thesis, Stanford Univ., CA.
- Kuulkers E., in 't Zand J. J. M., Atteia J.-L., Levine A. M., Brandt S., Smith D. A., Linares M., Falanga M., Sánchez-Fernández C., Markwardt C. B., Strohmayer T. E., Cumming A., Suzuki M., 2010, *A&A*, 514, A65
- Lamb F. K., Miller M. C., 2001, *ApJ*, 554, 1210
- Lapidus I. I., Sunyaev R. A., 1985, *MNRAS*, 217, 291
- Lowell A. W., Tomsick J. A., Heinke C. O., Bodaghee A., Boggs S. E., Kaaret P., Chaty S., Rodriguez J., Walter R., 2012, *ApJ*, 749, 111
- Méndez M., van der Klis M., Ford E. C., Wijnands R., van Paradijs J., 1999, *ApJL*, 511, L49
- Messenger C., Bulten H. J., Crowder S. G., Dergachev V., Galloway D. K., Goetz E., Jonker R. J. G., Lasky P. D., Meadors G. D., Melatos A., Premachandra S., Riles K., Sammut L., Thrane E. H., Whelan J. T., Zhang Y., 2015, *PRD*, 92, 023006
- Miller M. C., Lamb F. K., 2016, *European Physical Journal A*, 52, 63
- Miller M. C., Lamb F. K., Psaltis D., 1998, *ApJ*, 508, 791
- Muno M. P., Chakrabarty D., Galloway D. K., Savov P., 2001, *ApJL*, 553, L157
- Muno M. P., Galloway D. K., Chakrabarty D., 2004, *ApJ*, 608, 930
- Natalucci L., Cornelisse R., Bazzano A., Cocchi M., Ubertini P., Heise J., in 't Zand J. J. M., Kuulkers E., 1999, *ApJL*, 523, L45
- Patruno A., Watts A. L., 2012, *ArXiv e-prints*
- Piro A. L., Bildsten L., 2007, *ApJ*, 663, 1252
- Popham R., Sunyaev R., 2001, *ApJ*, 547, 355
- Psaltis D., 2001, *Advances in Space Research*, 28, 481
- Revnivtsev M., 2003, *A&A*, 410, 865
- Revnivtsev M., Sazonov S., Gilfanov M., Churazov E., Sunyaev R., 2006, *A&A*, 452, 169
- Revnivtsev M. G., Gilfanov M. R., 2006, *A&A*, 453, 253
- Shakura N. I., Sunyaev R. A., 1988, *Advances in Space Research*, 8, 135
- Sibgatullin N. R., Sunyaev R. A., 1998, *Astronomy Letters*, 24, 774
- Sibgatullin N. R., Sunyaev R. A., 2000, *Astronomy Letters*, 26, 699
- Smarr L. L., Blandford R., 1976, *ApJ*, 207, 574
- Stella L., Vietri M., 1999, *Physical Review Letters*, 82, 17
- Strohmayer T., Bildsten L., 2006, *New views of thermonuclear bursts*. pp 113–156
- Strohmayer T. E., Markwardt C. B., Kuulkers E., 2008, *ApJL*, 672, L37
- Strohmayer T. E., Markwardt C. B., Swank J. H., in 't Zand J., 2003, *ApJL*, 596, L67
- Strohmayer T. E., Zhang W., Swank J. H., Smale A., Titarchuk L., Day C., Lee U., 1996, *ApJL*, 469, L9
- Stuchlík Z., Konar S., Miller J. C., Hledík S., 2008, *A&A*, 489, 963
- Suleimanov V., Poutanen J., 2006, *MNRAS*, 369, 2036

- Sunyaev R. A., Titarchuk L., 1989, in Hunt J., Batrick B., eds, *Two Topics in X-Ray Astronomy, Volume 1: X Ray Binaries. Volume 2: AGN and the X Ray Background* Vol. 296 of ESA Special Publication, X ray burster spectra in the state of the persistent flux level. Two temperature models of the neutron star atmosphere. pp 627–631
- Thompson T. W. J., Rothschild R. E., Tomsick J. A., Marshall H. L., 2005, *ApJ*, 634, 1261
- van der Klis M., 2000, *ARA&A*, 38, 717
- van der Klis M., 2006, *Rapid X-ray Variability*. pp 39–112
- van der Klis M., Swank J. H., Zhang W., Jahoda K., Morgan E. H., Lewin W. H. G., Vaughan B., van Paradijs J., 1996, *ApJL*, 469, L1
- Wang D. H., Chen L., Zhang C. M., Lei Y. J., Qu J. L., 2014, *Astronomische Nachrichten*, 335, 168
- Watts A. L., 2012, *ARA&A*, 50, 609
- Wijnands R., van der Klis M., 1998, *Nature*, 394, 344
- Zhang C., 2004, *A&A*, 423, 401
- Zhang W., Jahoda K., Kelley R. L., Strohmayer T. E., Swank J. H., Zhang S. N., 1998, *ApJL*, 495, L9

This paper has been typeset from a \TeX / \LaTeX file prepared by the author.